Journal of Clinical and Translational Hepatology **2026**
DOI: 10.14218/JCTH.2025.00689

Research Letter

FN1 Knockout Inhibits Tumorigenesis but Promotes Lung Metastasis in Hepatocellular Carcinoma

Meng Han[1], Xin Liu[2], Jian-Jun Gou[1] and Feng-Min Lu[2*]

[1]Department of Laboratory Medicine, The First Affiliated Hospital of Zhengzhou University, Zhengzhou, Henan, China; [2]Department of Microbiology & Infectious Disease Research Center, School of Basic Medical Sciences, Peking University Health Science Center, Beijing, China

Received: December 16, 2025 | **Revised:** May 05, 2026 | **Accepted:** June 09, 2026 | **Published online:** July 2, 2026

Citation of this article: Han M, Liu X, Gou JJ, Lu FM. FN1 Knockout Inhibits Tumorigenesis but Promotes Lung Metastasis in Hepatocellular Carcinoma. J Clin Transl Hepatol 2026. doi: 10.14218/JCTH.2025.00689.

Primary liver cancer is the sixth most common malignancy globally and ranks as the third leading cause of cancer-related deaths, posing a persistent public health burden with limited effective treatment options.[1] Hepatocellular carcinoma (HCC), the predominant histologic subtype, accounts for approximately 90% of primary liver cancer,[2] with hepatitis B virus (HBV) infection being a major etiological factor. The poor prognosis of HCC is largely due to its late diagnosis and high metastatic propensity for intrahepatic or extrahepatic metastasis, which often leads to the loss of the optimal window for surgical intervention.[3] Therefore, identifying key regulatory molecules that influence the development of HCC is crucial.

Fibronectin (FN1), a multifunctional extracellular matrix (ECM) glycoprotein, is involved in embryogenesis, wound healing, and tissue remodeling.[4] Although FN1 is generally oncogenic in most solid tumors by remodeling the ECM and activating integrin-driven pathways, its deficiency paradoxically impairs collagen barriers and facilitates cell detachment, thereby promoting metastasis.[5–10] Thus, this duality of FN1 is not contradictory but rather context-dependent, varying with tumor stage, tissue microenvironment, and the balance between mechanotransduction and immunomodulation. However, HBV DNA integration into FN1 occurs preferentially in adjacent non-cancerous tissues rather than in tumor tissues, a finding that appears to contradict the established pro-oncogenic function of FN1.[11] Accordingly, clarifying the role of FN1 in HCC is of paramount importance.

Plasmid construction: The sgRNA/Cas9 dual-expression vector pSpCas9(BB)-2A-GFP (PX458) was sourced from Addgene (Cambridge, MA). The sgP53/Pten dual-cassette plasmid was constructed as described previously.[12] The sgFn1 dual-cassette plasmids were generated following the same strategy. For clarity, all plasmids are referred to throughout this study as follows: sgP53/Pten, sgFn1(1+4), sgFn1(1+3), sgFn1(2+4), sgFn1(2+3), and vector. The following sequences are four sgRNAs targeting the Fn1 gene and primer sequences (5′-3′): sgRNA1: AACCAGGGCGTTGCCTAGGT; sgRNA2: GGGTTTTAACTGCGAGAGCA; sgRNA3: TGATCTGGGACTGTACCTGC; sgRNA4: GGGGGTCAGTCCTACAAGAT; F: AGGTAGTTCCCCTGCCCATA; R: CTCGCAGCACATTTCACTGG.

Culture of cells: The origin and specific culture methods for Hepa1-6 cells and those for H2.35 cells were as described previously.[12,13]

Cell transfection and monoclonal screening: Hepa1-6 cells were seeded at a density of 2×10^5 cells per 3.5-cm culture dish. When cells confluence reached approximately 70%, transfection was performed using the sgFn1(1+4) plasmid. After visible colonies formed in 96-well plates, GFP-positive clones were selected under a fluorescence microscope and expanded for further culture. Successful Fn1 knockout (Fn1-KO) was confirmed by Western blot analysis.

Functional assays: CCK-8, colony formation, cell migration, cell invasion, and cell adhesion assays were carried out as previously described.[14,15] The collagen used was Collagen Type I Rat Tail (Corning, 354236), at a concentration of 5 μg/cm^2.

Animal experiments: C57BL/6J mice and HBV transgenic mice on a C57BL/6 genetic background were sourced from Peking University Health Science Center. All animals were housed under specific pathogen-free conditions in individually ventilated cages within the institution's Department of Laboratory Animal Science. All experimental procedures were approved by the Institutional Animal Care and Use Committee of Peking University Health Science Center (LA2021492). All animal experiments were conducted in accordance with institutional guidelines for the care and use of laboratory animals. The procedure for hydrodynamics-based tail vein injection of plasmids and the post-injection care of mice were performed as described previously.[12,16]

Subcutaneous tumor implantation: A 100 μL PBS suspension containing 1×10^6 Hepa1-6 cells (wild-type (WT), Fn1-KO cell lines #5 and #13) was inoculated into each mouse's axillary region. Each group had five mice. The mice were not pregrouped but were randomly assigned to three groups during inoculation. Once palpable tumors were observed, tumor volume was monitored every two days. Measurements were taken six times before the mice were sacrificed.

Western blot: The procedures for Western blotting were conducted as described previously.[12] Antibody details are

[*]**Correspondence to:** Feng-Min Lu, Department of Microbiology & Infectious Disease Research Center, School of Basic Medical Sciences, Peking University Health Science Center, Beijing 100083, China. ORCID: https://orcid.org/0000-0002-1832-3209. Tel/Fax: +86-10-82805136, E-mail: lu.fengmin@hsc.pku.edu.cn.

listed in Supplementary Table 1. Flow cytometric analysis of tumor tissues: The procedures for flow cytometry were conducted as described previously.[13] Antibody details are listed in Supplementary Table 1. Analysis of immune cell infiltration and RNA-seq: The TCGA-LIHC dataset was acquired from the Genomic Data Commons portal (https://portal.gdc.cancer.gov). Following normalization of the raw expression data, immune cell infiltration analysis was conducted using the SangerBox platform.[17] RNA sequencing was performed following established protocols. Transcriptomic data were analyzed for differentially expressed genes, followed by Gene Ontology enrichment and Gene Set Enrichment Analysis. Subsequent signaling pathway analyses focused on subcutaneous tumors derived from Fn1-KO and WT Hepa1-6 cells.

Immunohistochemistry and multicolor immunohistochemistry: The procedures for immunohistochemistry and multicolor immunohistochemistry were conducted as described previously.[13] Antibody details are listed in Supplementary Table 1.

Statistical analysis: All data in statistical graphs are presented as mean ± standard deviation, unless otherwise specified. Statistical analyses were performed using GraphPad Software (version 8.0) or R software (version 4.0.0). Unless otherwise indicated, an unpaired Student's t-test or one-way ANOVA was used for group comparisons. Two-tailed *P*-values < 0.05 were considered statistically significant.

To clarify these conflicting observations, we designed four sgRNAs targeting the murine *Fn1* gene and selected the sgFn1(1+4) dual-sgRNA combination for subsequent experiments (Supplementary Fig. 1A–E). Using monoclonal cell screening, we successfully established *Fn1*-KO Hepa1-6 cell strains (#5, #13, #18, and #19) (Fig. 1A). Functional experiments revealed that *Fn1*-KO cells showed markedly impaired proliferation, migration, invasion, and adhesion, with strains #5 and #13 exhibiting the most pronounced defects (Fig. 1B; Supplementary Fig. 1F–J). Notably, collagen supplementation failed to rescue the proliferation deficiency of *Fn1*-KO cells (Fig. 1C), although collagen alone could impair proliferation (Supplementary Fig. 1K). We then performed rescue experiments by overexpressing exogenous Fn1 in #5 and #13. CCK-8 proliferation assays showed that the proliferation rates were restored upon FN1 re-expression in both clones (Supplementary Fig. 1L–M). Moreover, xenograft tumors derived from *Fn1*-KO cells grew significantly more slowly in C57BL/6J mice than WT controls, with strain #5 displaying the strongest suppression (Fig. 1D–F). Further transcriptomic profiling (Supplementary Fig. 2A) and immunohistochemical analyses confirmed concomitant downregulation of types I and III collagen in *Fn1*-deficient tumors (Supplementary Fig. 2B), which might partly explain the observed functional impairments in these *Fn1*-KO cells.

Regarding the immunosuppressive microenvironment of HCC,[18] bioinformatic interrogation of public datasets revealed that high FN1 expression in HCC correlated with increased infiltration of M2 macrophages and reduced recruitment of $CD8^+$ T cells (Supplementary Fig. 2C–F). Consistent with this, flow cytometry demonstrated a decreased proportion of total and M2 macrophages (Fig. 1G; Supplementary Fig. 2G), along with a reduction in PD-1^+ $CD8^+$ T cells (Fig. 1H; Supplementary Fig. 2H), in the xenograft tumor tissues from the *Fn1*-KO group. In addition, Gene Set Enrichment Analysis identified significant activation of interferon-stimulated genes and interferon-β responses upon *Fn1* deletion (Supplementary Fig. 2I).

To establish physiological relevance, we used HBV/S transgenic mice with *P53*/*Pten* deficiency.[12] *Fn1*-KO, accompanied by reduced ECM deposition, significantly attenuated hepatic tumor incidence and malignant progression arising from endogenous *P53*/*Pten* dual knockout (Fig. 1J–L; Supplementary Fig. 3A and B). Multicolor immunohistochemistry revealed a reduction in M2 macrophages and PD-1^+ $CD8^+$ T cells in the tumor tissues of the *Fn1*-KO group (Supplementary Fig. 3C). Intriguingly, despite the decreased incidence of primary tumors, the number of pulmonary metastatic tumors characterized by lower FN1 expression remained comparable between the P53/Pten/Fn1-KO group and the *P53*/*Pten* dual-KO group (Fig. 1M; Supplementary Fig. 3D).

As the organ with the highest FN1 expression, the liver presents a unique context for FN1 function.[19] Our findings support a tumor-promoting role for FN1 in HBV-related HCC. Mechanistically, *FN1* deficiency profoundly altered ECM composition in our models, with collagen reduction indicating microenvironmental remodeling. In addition, FN1 may facilitate HCC progression by increasing the infiltration of M2 macrophages and PD-1^+ $CD8^+$ T cells.

Although prior reports described FN1's proliferative effects *in vitro*,[3,20] its role in tumorigenesis remains undefined, particularly in HCC. Here, our results demonstrate that Fn1-KO significantly reduces hepatocarcinogenesis, supporting its tumor-promoting role. Mechanistically, FN1 promotes collagen deposition via the TGF-β/PI3K/Akt pathway,[5,8,9] and mediates ECM-cytoskeleton signaling through integrin α5β1 to activate the FAK/PI3K/Akt proliferation axis.[21,22] However, Fn1-KO permanently disrupts this integrin-mediated mechanotransduction, explaining why exogenous collagen supplementation failed to rescue the proliferative capacity of FN1-deficient cells.[23,24] Paradoxically, we observed increased trend of pulmonary metastasis with diminished FN1 expression in metastatic cells. In line with a previous report that high FN1 expression can suppress metastasis,[25] our *in vitro* study showed that FN1 deletion compromised adhesion and consequently facilitated lung metastasis of malignant tumor cells, possibly due to the unique alveolar architecture lacking vascular constraints. In clinical practice, lower expression of FN1 in primary HCC tissue indicates a higher risk of distant lung metastasis; therefore, closer monitoring with pulmonary imaging should be implemented to rule out early-stage lung metastasis in such patients.

In conclusion, this study demonstrates that FN1 deficiency suppresses hepatocyte malignant transformation and HCC progression but promotes pulmonary metastasis.

Supporting information

Supplementary material for this article is available at https://doi.org/10.14218/JCTH.2025.00689.

Funding

None to declare.

Conflict of interest

FML has been an Editorial Board Member of *Journal of Clinical and Translational Hepatology* since 2013. The other authors have no conflict of interests related to this publication.

Author contributions

Conceptual design of the study (FML), data collection (MH, XL, JJG), statistical analysis, and writing of the original draft (MH, XL, FML). All authors reviewed and approved the final version and publication of the manuscript.

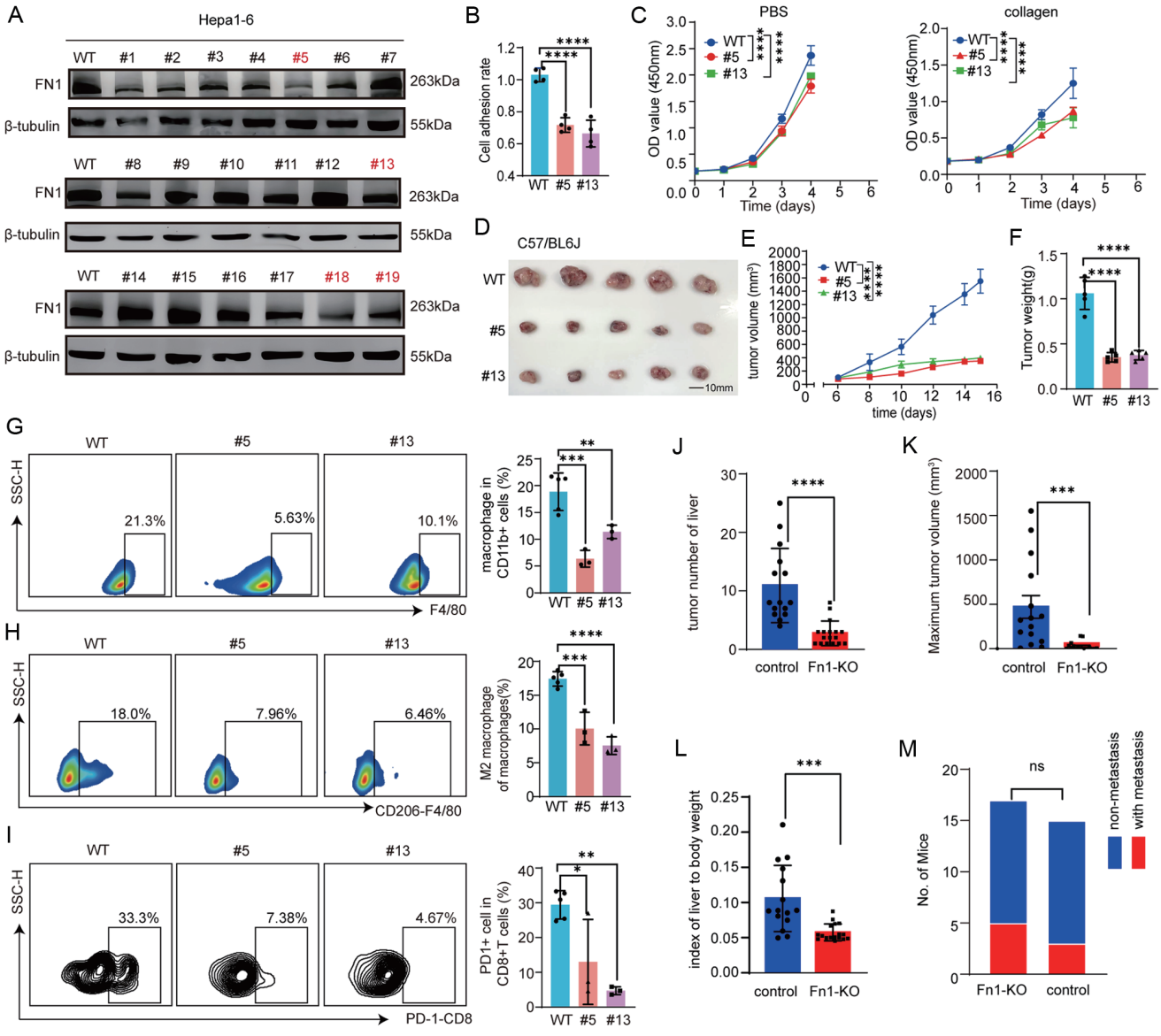

Fig. 1. Assessment of primary tumor formation and lung metastasis following FN1 knockout in hepatocellular carcinoma. (A) Western blot analysis of FN1 protein expression in 19 monoclonal *Fn1*-knockout (*Fn1*-KO) Hepa1-6 cell lines (#1–#19). (B) Cell adhesion assay comparing wild-type (WT) and *Fn1*-KO Hepa1-6 cells (n = 4). (C) Proliferation of WT and *Fn1*-KO Hepa1-6 cells cultured on collagen- or PBS-coated plates (n = 4). (D) Representative images of subcutaneous tumors in C57BL/6J mice inoculated with WT or *Fn1*-KO Hepa1-6 cells (n = 5). (E) Tumor weight in C57BL/6J mice inoculated with WT or *Fn1*-KO Hepa1-6 cells (n = 5). (F) Tumor growth curves in C57BL/6J mice inoculated with WT or *Fn1*-KO Hepa1-6 cells (n = 5). (G–I) Flow cytometric analysis of tumor-infiltrating immune cells (WT, n = 5; #5, n = 3; #13, n = 3): (G) total macrophages, (H) M2 macrophages, (I) PD-1$^+$ CD8$^+$ T cells. (J–L) Spontaneous HCC model in HBV transgenic mice: (J) quantification of liver surface tumor numbers in each group. n = 15 for the control group and n = 17 for the Fn1-KO group; (K) maximum tumor volume; (L) liver/body weight ratio (control, n = 15; *Fn1*-KO, n = 17). Control: Reprogrammed mice were administered sgP53/Pten + empty vector plasmid via tail vein injection. Fn1-KO: Reprogrammed mice were administered sgP53/Pten + sgFn1(1+4) via tail vein injection. (M) Lung metastasis incidence. Data in (K) are presented as mean ± SEM; all other data represent mean ± SD. Significance was determined by Student's *t*-test (B, F, G–L), two-way ANOVA (C, E), or chi-square test (M); **P* < 0.05, ***P* < 0.01, ****P* < 0.001, *****P* < 0.0001, ns, no significance. HCC, hepatocellular carcinoma; Fn1-KO, Fn1 knockout; PBS, phosphate-buffered saline; WT, wild-type.

Ethical statement

All experimental procedures were approved by the Institutional Animal Care and Use Committee of Peking University Health Science Center (LA2021492). All animal experiments were conducted in accordance with institutional guidelines for the care and use of laboratory animals. All animals received human care. The use of public TCGA-LIHC data did not require additional ethical approval or informed consent because all data were publicly available and de-identified.

Data sharing statement

The RNA-seq data used to support the findings of this study are available from the corresponding author.

References

[1] Sung H, Ferlay J, Siegel RL, Laversanne M, Soerjomataram I, Jemal A, *et al*. Global Cancer Statistics 2020: GLOBOCAN Estimates of Incidence and Mortality Worldwide for 36 Cancers in 185 Countries. CA Cancer J Clin 2021;71(3):209–249. doi:10.3322/caac.21660, PMID:33538338.

[2] Llovet JM, Kelley RK, Villanueva A, Singal AG, Pikarsky E, Roayaie S, *et al*. Hepatocellular carcinoma. Nat Rev Dis Primers 2021;7(1):6. doi:10.1038/s41572-020-00240-3, PMID:33479224.
[3] Liu HH, Xu Y, Li CJ, Hsu SJ, Lin XH, Zhang R, *et al*. An SCD1-dependent mechanoresponsive pathway promotes HCC invasion and metastasis through lipid metabolic reprogramming. Mol Ther 2022;30(7):2554–2567. doi:10.1016/j.ymthe.2022.03.015, PMID:35358687.
[4] Schwarzbauer JE, DeSimone DW. Fibronectins, their fibrillogenesis, and in vivo functions. Cold Spring Harb Perspect Biol 2011;3(7):a005041. doi:10.1101/cshperspect.a005041, PMID:21576254.
[5] Zhang H, Chen X, Xue P, Ma X, Li J, Zhang J. FN1 promotes chondrocyte differentiation and collagen production via TGF-β/PI3K/Akt pathway in mice with femoral fracture. Gene 2021;769:145253. doi:10.1016/j.gene.2020.145253, PMID:33098939.
[6] Zhang L, Zhang C, Xing Z, Lou C, Fang J, Wang Z, *et al*. Fibronectin 1 derived from tumor-associated macrophages and fibroblasts promotes metastasis through the JUN pathway in hepatocellular carcinoma. Int Immunopharmacol 2022;113(Pt A):109420. doi:10.1016/j.intimp.2022.109420, PMID:36461607.
[7] Shinde A, Libring S, Alpsoy A, Abdullah A, Schaber JA, Solorio L, *et al*. Autocrine Fibronectin Inhibits Breast Cancer Metastasis. Mol Cancer Res 2018;16(10):1579–1589. doi:10.1158/1541-7786.MCR-18-0151, PMID:29934326.
[8] Zollinger AJ, Smith ML. Fibronectin, the extracellular glue. Matrix Biol 2017;60-61:27–37. doi:10.1016/j.matbio.2016.07.011, PMID:27496349.
[9] Saunders JT, Schwarzbauer JE. Fibronectin matrix as a scaffold for procollagen proteinase binding and collagen processing. Mol Biol Cell 2019;30(17):2218–2226. doi:10.1091/mbc.E19-03-0140, PMID:31242089.
[10] Zhang M, He M, Du F, Xie Y, Liao Y, Pan X. Macrophage-derived FN1 promotes peritoneal cavity metastasis of gastric cancer by inhibiting the Hippo signaling pathway via SDC4. Biochim Biophys Acta Mol Cell Res 2026;1873(1):120063. doi:10.1016/j.bbamcr.2025.120063, PMID:41005547.
[11] Li X, Zhang J, Yang Z, Kang J, Jiang S, Zhang T, *et al*. The function of targeted host genes determines the oncogenicity of HBV integration in hepatocellular carcinoma. J Hepatol 2014;60(5):975–984. doi:10.1016/j.jhep.2013.12.014, PMID:24362074.
[12] Liu Y, Qi X, Zeng Z, Wang L, Wang J, Zhang T, *et al*. CRISPR/Cas9-mediated p53 and Pten dual mutation accelerates hepatocarcinogenesis in adult hepatitis B virus transgenic mice. Sci Rep 2017;7(1):2796. doi:10.1038/s41598-017-03070-8, PMID:28584302.
[13] Liu X, Yang D, Jiang Q, Han M, Zhou Z, Li Y, *et al*. Tumor Cell-Derived CXCL2 Potentiates Neutrophil-Mediated Antitumor Immunity by Inhibiting Cholesterol Biosynthesis in Hepatocellular Carcinoma. Adv Sci (Weinh) 2026;13(2):e11436. doi:10.1002/advs.202511436, PMID:41114470.
[14] Lin R, Bao X, Wang H, Zhu S, Liu Z, Chen Q, *et al*. TRPM2 promotes pancreatic cancer by PKC/MAPK pathway. Cell Death Dis 2021;12(6):585. doi:10.1038/s41419-021-03856-9, PMID:34099637.
[15] Zhang Z, Zhu H, Zhao G, Miao Y, Zhao L, Feng J, *et al*. Programmable and Reversible Integrin-Mediated Cell Adhesion Reveals Hysteresis in Actin Kinetics that Alters Subsequent Mechanotransduction. Adv Sci (Weinh) 2023;10(35):e2302421. doi:10.1002/advs.202302421, PMID:37849221.
[16] Goel F, Giri A, Kumar D, Pal A, Singh P. Comparative information of different animal models used in chronic diseases. In: Rai SN, Singh SK, Singh V (eds). Advancements in Modeling-Based Therapeutics and Technology for Chronic Diseases. New York, US: Academic Press; 2026:51–84.
[17] Chen D, Xu L, Xing H, Shen W, Song Z, Li H, *et al*. Sangerbox 2: Enhanced functionalities and update for a comprehensive clinical bioinformatics data analysis platform. Imeta 2024;3(5):e238. doi:10.1002/imt2.238, PMID:39429873.
[18] Cai J, Song L, Zhang F, Wu S, Zhu G, Zhang P, *et al*. Targeting SRSF10 might inhibit M2 macrophage polarization and potentiate anti-PD-1 therapy in hepatocellular carcinoma. Cancer Commun (Lond) 2024;44(11):1231–1260. doi:10.1002/cac2.12607, PMID:39223929.
[19] Duff MO, Olson S, Wei X, Garrett SC, Osman A, Bolisetty M, *et al*. Genome-wide identification of zero nucleotide recursive splicing in Drosophila. Nature 2015;521(7552):376–379. doi:10.1038/nature14475, PMID:25970244.
[20] Jha RK, Ma Q, Chen S, Sha H, Ding S. Relationship of fibronectin and CD44v6 expression with invasive growth and metastasis of liver cancer. Cancer Invest 2009;27(3):324–328. doi:10.1080/07357900802375753, PMID:19194823.
[21] Singh P, Carraher C, Schwarzbauer JE. Assembly of fibronectin extracellular matrix. Annu Rev Cell Dev Biol 2010;26:397–419. doi:10.1146/annurev-cellbio-100109-104020, PMID:20690820.
[22] Pal S, Ganguly KK, Chatterjee A. Extracellular matrix protein fibronectin induces matrix metalloproteinases in human prostate adenocarcinoma cells PC-3. Cell Commun Adhes 2013;20(5):105–114. doi:10.3109/15419061.2013.833193, PMID:24047237.
[23] Li B, Shen W, Peng H, Li Y, Chen F, Zheng L, *et al*. Fibronectin 1 promotes melanoma proliferation and metastasis by inhibiting apoptosis and regulating EMT. Onco Targets Ther 2019;12:3207–3221. doi:10.2147/OTT.S195703, PMID:31118673.
[24] Ji Z, Li X, Wang Y, Zhang X, Yang Z, Zhang Y, *et al*. Fibronectin 1 Aggravates Colon Cancer Metastasis by Regulating RAP1B Protein Stability Through Akt/CREB Signalling Pathway. J Cell Mol Med 2025;29(13):e70702. doi:10.1111/jcmm.70702, PMID:40638546.
[25] Glasner A, Levi A, Enk J, Isaacson B, Viukov S, Orlanski S, *et al*. NKp46 Receptor-Mediated Interferon-γ Production by Natural Killer Cells Increases Fibronectin 1 to Alter Tumor Architecture and Control Metastasis. Immunity 2018;48(2):396–398. doi:10.1016/j.immuni.2018.01.010, PMID:29466761.